Compression of the $B2$ high-pressure phase of NaCl

Dion L. Heinz and Raymond Jeanloz
Department of Geology and Geophysics, University of California, Berkeley, Berkeley, California 94720
(Received 6 August 1984)

Results from room-temperature static-compression experiments are presented for the $B2$ phase of NaCl between 25 and 70 GPa (250—700 kbar) pressure. The volume and bulk modulus of the $B2$ phase, extrapolated to zero pressure, are $V_{02}/V_{01}=0.929(\pm 0.071)$ and $K_{02}=36.2(\pm 4.2)$ GPa based on a finite-strain analysis of the new data (V_{01} is the zero-pressure volume of the $B1$ phase). Our results are in good agreement with *ab initio* calculations of the NaCl ($B2$) equation of state. Also, we find that the bulk modulus probably decreases across the $B1$-$B2$ transition, in accord with previous predictions. We illustrate the use of high-pressure compression studies on different polymorphs for empirically determining interatomic potentials of ionic crystals.

INTRODUCTION

Sodium chloride, being a model of ionic bonding, is one of the most thoroughly studied solids, both experimentally and theoretically. Recent advances in high-pressure experimentation, by way of the diamond cell, have made it possible to determine the isothermal compression of the $B2$ phase (CsCl structure) of NaCl, which is only stable above 30 GPa (300 kbar).[1] This is of considerable interest because the equation of state of the low-pressure $B1$ phase (NaCl structure) is well known,[2] and the influence of crystal structure on the elasticity of NaCl can therefore be experimentally determined. Similarly, recent *ab initio* calculations on the $B1$ and $B2$ phases of NaCl provide insights into the relationship between crystal structure and properties.[3-4] The calculations reproduce many of the properties of the $B1$ phase; however, a significant deviation was noted with the previously measured equation of state of the $B2$ phase:[3-4] Either the existing data are biased or the theoretical results are significantly less accurate for the high-pressure structure than for the low-pressure structure. Consequently, we undertook the present study in order to clarify the disagreement between theoretical and experimental results for the high-pressure phase of NaCl.

EXPERIMENTAL PROCEDURE

Polycrystalline NaCl (obtained from Alpha Ventron, 99.5% purity, and Malinckrodt, 99.99% purity) was compressed at room temperature with a Mao-Bell—type diamond cell.[5] The samples were gasketed, and the pressure was determined by the ruby-fluorescence technique[6] using the system described by Jeanloz.[7] We used a fine ruby powder for the pressure measurements, which were made in each run on at least six different spots over the surface of the sample. The quoted pressure is determined from the areal average of the measurements, and the uncertainties are estimated by taking one standard deviation of the measured values. Sample 1*c* was laser heated to ~2000 K after run 14 and then x-rayed again to obtain run 12 (Table I). The change in pressure between these two points reflects an annealing out of some of the nonhydrostatic pressure gradient across the sample. Also, a variety of pressure transmitting media were used in the present experiment in order to document the effects of nonhydrostaticity (finite shear strength of the pressure medium): FeO, mineral oil, and NaCl (i.e., no separate medium). Within the resolution of the data, there is no obvious nonhydrostatic effect on the compression measurements.

Lattice parameters of the samples at high pressure and room temperature were determined by x-ray diffraction using Mo $K\alpha$ radiation [$\lambda(\bar{\alpha})=71.073$ pm]. Using a rotating anode generator and films in the Debye-Scherrer configuration, typical exposures were 24—72 h long depending upon whether or not a Zr filter or a monochromator was used. The sample-to-film distance was determined by placing a gold sample in the diamond cell at zero pressure (without a pressure medium), and the lattice parameter of the $B2$ phase was determined from the 110 diffraction line. Errors in the volume (one standard deviation) were estimated from the variation among four readings of the diffraction line and the uncertainty in the sample-to-film distance.

RESULTS

The new static-compression results for the $B2$ phase of NaCl are listed in Table I and are shown in Fig. 1. All data but one were collected above 32 GPa, and no diffraction lines of the $B1$ phase were observed in any of the runs [the $B1$-$B2$ transition occurs at 29 ± 3 GPa in NaCl (Ref. 1)]. The one run below the equilibrium transition pressure (number 1) was made on decompression so that the high-pressure phase was maintained metastably.

For comparison, the isotherm of the $B1$ phase of NaCl is included in Fig. 1. It is evident that the equations of state of the two polymorphs are almost indistinguishable because of the small volume change at the transition: $\Delta V/V_{tr}=0.013$ at 29 GPa (given the uncertainties in the compression curves of both phases, 1 to 2% in volume,

TABLE I. NaCl $B2$ phase: static-compression data.

Run number	Sample[a]	Pressure (GPa)	V/V_{01}[b]
1	1c	24.5(±3.7)	0.6653(±0.0030)
2	2e	32.2(±2.6)	0.6107(±0.0014)
3	2d	32.3(±3.1)	0.6042(±0.0018)
4	2d	32.3(±3.6)	0.6165(±0.0012)
5	2e	43.9(±3.7)	0.5837(±0.0027)
6	2d	47.0(±5.0)	0.5632(±0.0012)
7	2e	49.0(±2.9)	0.5701(±0.0017)
8	2e	50.4(±3.4)	0.5612(±0.0017)
9	2d	52.0(±5.4)	0.5535(±0.0016)
10	1a	58.9(±1.8)	0.5505(±0.0016)
11	1b	60.5(±3.6)	0.5430(±0.0016)
12	1c	64.3(±2.3)	0.5201(±0.0022)
13	1c	64.9(±3.3)	0.5144(±0.0013)
14	1c	68.9(±3.7)	0.5253(±0.0014)

[a]Numbers indicate diamond cell used, letters indicate sample. The pressure medium was FeO for samples *a*, *b*, and *c*; no pressure medium was used for sample *d*, and mineral oil was used for sample *e*.
[b]Volume V is referenced to the zero-pressure volume of the $B1$ phase, V_{01}.

this value is compatible with the *in situ* determination of Liu and Bassett[8]). The change in volume for NaCl at the $B1$-$B2$ transition is much smaller than is found among the other alkali halides (typically 9—17%).[1,8,9] This is a major reason for the high transition pressure of NaCl compared to those of the other alkali halides (below 2 GPa, except for the fluorides).

The $B2$ equation of state derived from pseudopotential,[3(a)] modified electron gas (MEG),[3(b)] and augmented plane wave[4] (APW) calculations are in good agreement with each other and also compare favorably with the data. In particular, the compressibility is well matched by the theoretical results over the observed range of pressure, although there is a systematic offset, with the data lying about 5 GPa above the theoretical equations of state. We note that the data and *ab initio* calculations are in much closer accord for the $B1$ phase of NaCl (i.e., well within the uncertainty of the theory),[3-4] so it is curious that a systematic, albeit small, discrepancy should arise for the $B2$ phase.

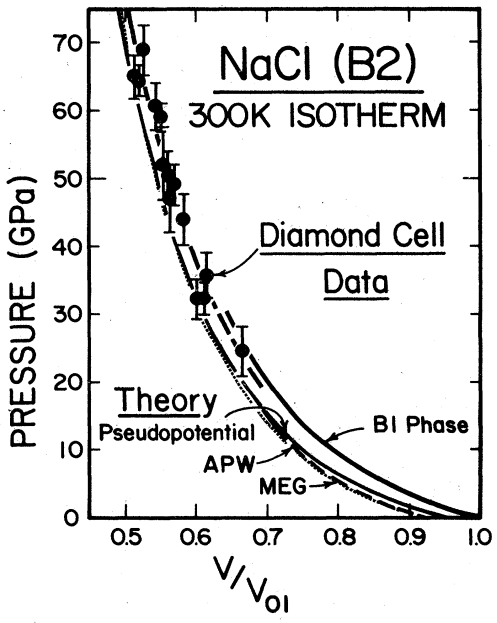

FIG. 1. Comparison of room-temperature static-compression data for the $B2$ phase of NaCl with compression curves. The solid circles with error bars and the heavy dashed line (unlabeled) represent the new diamond-cell measurements and the finite-strain fit to them. The heavy solid line labeled $B1$ phase is the experimentally constrained $B1$ equation (Ref. 2). The thin solid, dashed, and dotted curves are the pseudopotential [Ref. 3(a)], APW (Ref. 4), and MEG [Ref. 3(b)] results, respectively, corrected to 300 K.

Pressure and volume are relatively insensitive variables for making detailed comparisons of equations of state. Therefore, we turn to the finite-strain approach pioneered by Birch.[2,10] Because the $B2$ phase of NaCl cannot be retained to zero pressure, however, we obtain an equation of state from our data based on a finite-strain analysis for high-pressure phases.[11]

First, the pressure (P)-volume (V) data are recast in terms of a normalized stress

$$G=\frac{P}{3(1+2g)^{5/2}} \tag{1}$$

and a strain parameter

$$g=\tfrac{1}{2}[(V/V_{01})^{-2/3}-1]\ . \tag{2}$$

Then, the data are fitted to the finite-strain expansion of the stress G, which is simply a polynomial in the strain:

$$G=a+bg+cg^2+\cdots\ . \tag{3}$$

The coefficients are, to third order in strain,

$$\begin{aligned} a&=[(\alpha^2-1)/2]\alpha^5K_{02}[1+\xi(1-\alpha^2)]\ ,\\ b&=\alpha^7K_{02}[1+2\xi(1-\alpha^2)]\ ,\\ c&=-2\alpha^9K_{02}\xi\ , \end{aligned} \tag{4}$$

where K is the bulk modulus, and subscripts 0, 1, and 2

indicate zero pressure, the low-pressure phase, and the high-pressure phase, respectively. The zero-pressure volume, bulk modulus, and its pressure derivative (indicated by a prime) for the high-pressure phase are derived from the equation of state (3) by way of (4) and

$$\alpha=(V_{02}/V_{01})^{1/3},\quad \xi=\tfrac{3}{4}(4-K'_{02})\,. \tag{5}$$

The slope and curvature of the normalized stress (G) versus strain (g) fit determine K_{02} and ξ, whereas the intercept gives the initial volume of the $B2$ phase relative to that of the $B1$ phase. Further details of the analysis, including weighting of data and propagation of errors, are given elsewhere.[11] In the present case, the quality of the data warrant no more than a straight-line fit, as can be seen in Fig. 2. This second order or Birch equation of state is equivalent to setting K'_{02} equal to 4. The weighted least-squares fit to our data is shown in the figure, and the resulting zero-pressure values for the $B2$ phase of NaCl are $V_{02}/V_{01}=0.929(\pm0.071)$ and $K_{02}=36.2(\pm4.2)$ GPa, with $K'_{02}=4$ assumed.

Despite the offset from the theoretically derived equations of state, the predicted zero-pressure volumes from APW, MEG, and pseudopotential calculations are in good agreement with the value extrapolated from our data. In both cases, however, the theoretical equations of state exhibit positive curvature in Fig. 2, implying that $K'_{02}>4$,

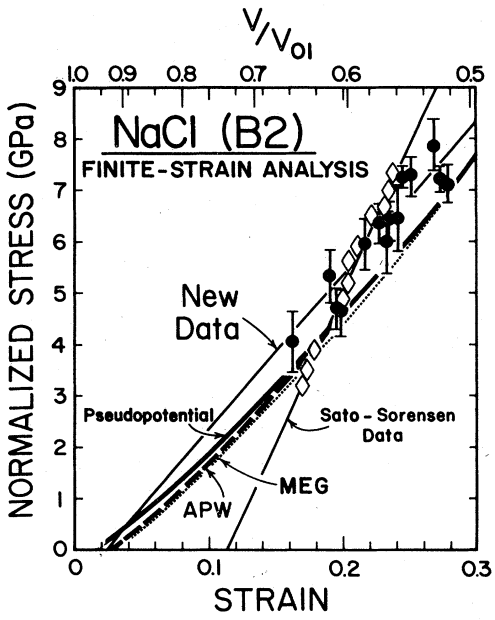

FIG. 2. Finite-strain analysis of several equations of state of the $B2$ phase of NaCl. The vertical and horizontal axes are normalized stress and strain, respectively (G and g as described in the text), and volume is shown on the upper scale (relative to the zero-pressure volume of the $B1$ phase). Solid circles with error bars indicate the data from this study, with the second-order finite-strain fit given by a thin solid line (new data). The diamonds and corresponding fit (Sato-Sorenson Data) are from Ref. 3(a) (bars excluded for clarity), and the three heavy lines (solid, dashed, and dotted) show the pseudopotential, APW, and MEG equations of state.

and thus yield a smaller K_{02} than our value (e.g., $K_{02}=26.6$ GPa and $K'_{02}=5.2$ according to Ref. 4). The theoretical equations of state slowly approach our second-order equation of state at pressures beyond 60 GPa.

The equations of state fitted to the NaCl data indicate that the bulk modulus decreases by about 6% at the transition from the $B1$ to the $B2$ phase, however, the uncertainty in this value is large ($\sim11\%$). This result qualitatively confirms the prediction, based on a lattice model, that the bulk modulus would decrease by about 8 to 12% at the $B1$-$B2$ transition of NaCl.[12] The prediction was based on the fact that although the volume (and hence the second-neighbor distance) decreases at the transition, there is an increase in the first-neighbor distance associated with the change in coordination. Analogous effects of coordination change on thermodynamic properties have been documented at $B1$-$B2$ transitions for a number of compounds.[12–15]

The previous diamond-cell data of Sato-Sorensen[1] are generally consistent with our new measurements, but it is clear that they lie on a systematically different trend. As a result, her equation of state extrapolates to a much smaller volume and a much larger bulk modulus for the $B2$ phase at zero pressure ($V_{02}/V_{01}=0.734\pm0.022$ and $K_{02}=121\pm23$ GPa, with $K'_{02}=4$ assumed). We believe that a systematic bias may have entered into Sato-Sorensen's equation of state due to bridging of the pressure-calibrating ruby chips between the diamond anvils, and possibly due to insufficient experimental distinction between the average pressure and the maximum pressure in each run.[16] In either case, too stiff an equation of state would result, as is observed.

Finally, we note that the properties of the $B2$ phase of NaCl may be thermodynamically ill defined at zero pressure because the lattice is expected to be mechanically unstable (with c_{44} vanishing at low pressures).[12] Therefore, meaningful comparisons between different theoretical and experimental results on this phase may be limited to high pressures.

EXPERIMENTALLY DETERMINED INTERIONIC POTENTIALS

Because of the differences in atomic packing geometry and interionic distances between the two structures, data for the $B1$ and $B2$ phases can be used to determine empirically the interatomic potential for NaCl. Why is this of interest, given that *ab initio* calculations successfully reproduce the properties of both phases, as shown above? The primary applications of analytical interionic potentials are for modeling lattice dynamics,[17] and liquid-state structures and dynamics.[18] Indeed, a number of structure-independent potential models have recently been proposed for just such applications to the alkali halides.[19–21]

For simplicity, we assume that a central, ionic pair potential applies to the two phases of NaCl. Unlike the traditional approach of Born and Mayer or Pauling, however, we need not assume a particular functional form for

the repulsive interaction; that interaction is given directly by the equations of state of the two phases. In this regard, our approach is the experimental analog of theoretical studies that have previously been made on the analytical form of the interatomic potential in alkali halides.[22–24] Furthermore, our approach yields the first structure-independent potentials that are based on data for different structures of the same compound. The structure independence of the potential is of particular importance for liquid state calculations.

The ionic pair potential is given as a sum of Coulombic and repulsive terms:

$$U=\frac{MZ_cZ_ae^2}{r}+\tfrac{1}{2}\sum_{i,j}u(\alpha_{ij}r)\ , \tag{6}$$

where M, Z, r, and e are the Madeulung constant, ion valence, first-neighbor distance, and charge on the electron, with subscripts c and a implying cation and anion. All nonelectrostatic interactions are included in the repulsive potential u, between ions i and j (separation r_{ij} given by $\alpha_{ij}r$).[25] Physically, the repulsive interactions are expected to decrease rapidly with increasing separation of the ions, and the sum in (6) converges rapidly. Thus, the pressure is given by differentiation of (6) as

$$P=P_{\text{Madelung}}+\frac{n_1}{3h}P_{\text{c-a}}(r)+\frac{n_2\alpha^3}{6h}P_{\text{a-a}}(\alpha r)+\cdots \tag{7}$$

with higher-order terms (contributions from cation-cation and more distant interactions) being assumed to be negligible; this assumption will be shown to be consistent with our results. The first- and second-neighbor coordination numbers and ratio of interionic distances, n_1, n_2, and $\alpha(\equiv r_{aa}/r)$, respectively, as well as the volume per ion pair divided by r^3 [$h=2$ and $8/(3\sqrt{3})$ for $B1$ and $B2$ structures] are explicitly shown in (7).

Defining a repulsive pressure which is a measurable function of r for each phase,

$$\begin{aligned}P_{\text{Rep}}&=\frac{3h}{n_1}(P-P_{\text{Madelung}})\\&=P_{\text{c-a}}+\frac{n_2\alpha^3}{2n_1}P_{\text{a-a}}(\alpha r)+\cdots\ .\end{aligned} \tag{8}$$

we use the equations of state of the $B1$ and $B2$ structures to determine the second-neighbor and higher-order contributions by way of the difference

$$\begin{aligned}\Delta P_{\text{Rep}}&=P^{B2}_{\text{Rep}}-P^{B1}_{\text{Rep}}\\&=3^{-1/2}P^{B2}_{\text{a-a}}(\alpha_{B2}r)-2^{3/2}P^{B1}_{\text{a-a}}(\alpha_{B1}r)+\cdots\ .\end{aligned} \tag{9}$$

The following abbreviations have been used in (7), (8), and (9):

$$P_{\text{Madelung}}=\frac{MZ_cZ_ae^2}{3hr^4}\ \text{and}\ P_{ij}(r_{ij})=\frac{-u(r_{ij})}{r_{ij}^2}\ ,$$

where a prime indicates differentiation. Note that it is the derivative of the repulsive potential, and not just its absolute value, that is constrained by the present approach.

The application of Eqs. (8) and (9) is illustrated in Fig. 3. Note that the repulsive interactions are larger in the $B2$ than in the $B1$ phase and, because of the normalization used to define P_{Rep} in (8), the difference between the curves for the two phases (ΔP_{Rep}) is a measure of the strength of the second- and more distant-neighbor interactions. Given the uncertainties in the experimental equations of state, we have not considered thermal corrections to reduce the data to static lattice conditions. The present analysis is sufficient, however, to document the usefulness of combining experimental data for two (or more) structures.

Our data are consistent with there being only a cation-anion contribution to the pressure in the $B1$ phase because extrapolation of the finite-strain equations of state for the two phases leads to a vanishing ΔP_{Rep} beyond a cation-anion distance of 300 pm (Fig. 3). This corresponds to the anion-anion repulsive interaction vanishing for separations exceeding 350 pm [cf. Fig. 4(b); negative values of $P_{\text{a-a}}$ are unphysical and hence not considered further]. The trouble with this conclusion is that it is based on an extrapolation far beyond the observed range of first-neighbor distances in either phase.

Alternatively, we derive a self-consistent and physically more plausible solution to (8) and (9) in which ΔP_{Rep}, and hence $P_{\text{a-a}}$, vanish smoothly at infinite separation. We assume an exponential decay with separation; however, the functional form used does not alter our qualitative conclusions. The result is a smooth cation-anion repulsive in-

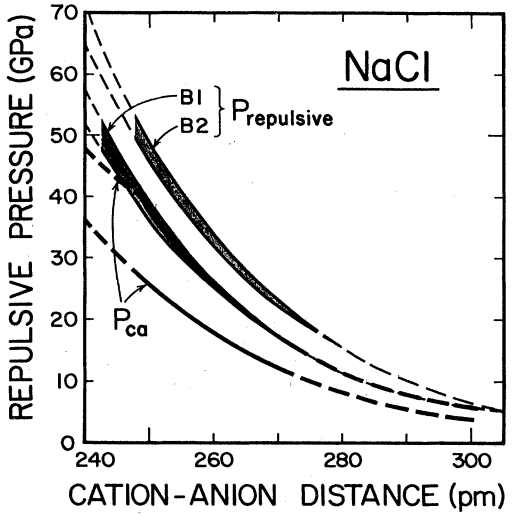

FIG. 3. Repulsive pressure vs cation-anion distance for NaCl. Curves and corresponding error envelopes $B1$ and $B2$ ($P_{\text{repulsive}}$) are the total repulsive pressure for each phase, dashed outside the observed ranges of cation-anion distance [cf. Eq. (8)]. The curves labeled $P_{\text{c-a}}$ represent the range of self-consistent solutions for the cation-anion contributions to the total repulsive pressure (see text for details).

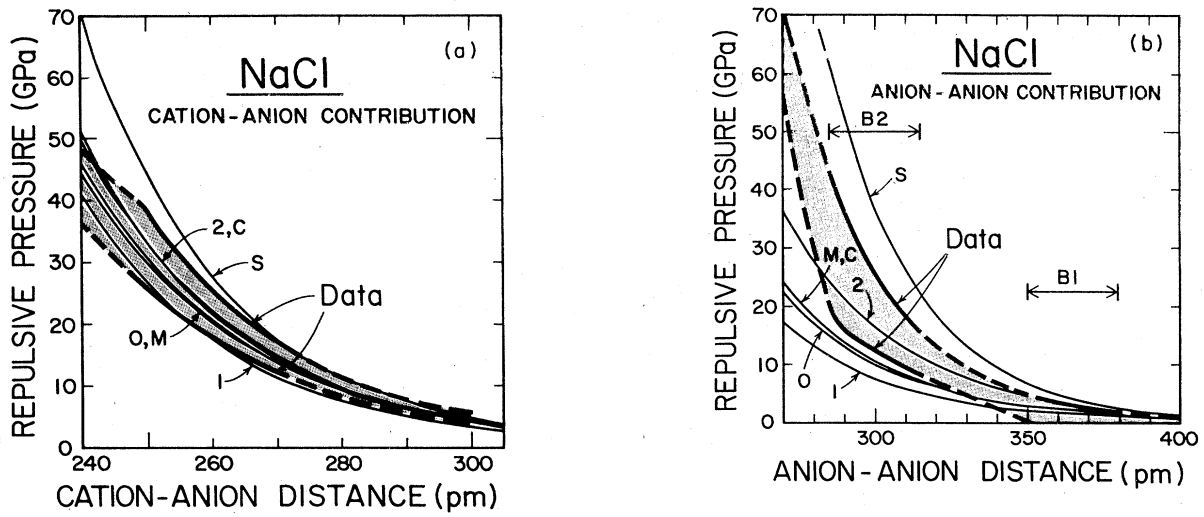

FIG. 4. Structure-independent potentials for NaCl plotted as repulsive pressure vs interionic-anion distances for (a) $P_{c\text{-}a}$ and (b) $P_{a\text{-}a}$. The shaded area between the two heavy curves represents the range of solutions illustrated in Fig. 3. For comparison, thin curves give structure-independent potentials from the literature (1, 2, Ref. 19; *S*, Ref. 20; *M*,*C*,*O*, Ref. 21).

teraction which is uniformly lower than in the first case because now there is a second-neighbor contribution that is substantial in the $B1$ phase, although still less than in the $B2$ phase at the same value of r (Fig. 3 and 4). The two models, with and without anion-anion interactions in the $B1$ phase, illustrate the range of potential models that would satisfy the data for the two structures of NaCl.

The interionic potentials derived from the data are compared in Fig. 4 with structure-independent potential models that have been recently proposed for NaCl.[19–21] For both first- and second-neighbor interactions, the *S* potential falls outside the experimental bounds. This is not surprising because the elastic constants predicted from the *S* potential are significantly larger than the observed values.[20] In contrast, the other potential models are in good agreement with the observed range of cation-anion repulsion [Fig. 4(a)]. What is interesting, however, is that these potentials all tend to underestimate the second-neighbor interactions in NaCl [Fig. 4(b)]. This deficiency in the models is made evident by the new equation-of-state measurement for the $B2$ phase.

SUMMARY

New isothermal compression data for the $B2$ phase of NaCl are in good agreement with results from *ab initio* calculations. Previous measurements appear to have been systematically biased, although there is general agreement with our present results. The effect of crystal structure on physical properties is demonstrated by the probable decrease in bulk modulus across the $B1$-$B2$ transition. Although unusual for high-pressure transformations, such a decrease is in accord with predictions based on a simple lattice model. Finally, we illustrate the use of measurements on different crystal structures for experimentally constraining the interionic repulsive forces.

ACKNOWLEDGMENT

These experiments were motivated by the theoretical results of S. Froyem and M. L. Cohen, as well as those of M. S. T. Bukowinski and J. Aidun. We thank them, R. Gordon, and Y. Sato-Sorenson for helpful discussions. This work was supported by NSF. R. Jeanloz was supported in part by the Alfred P. Sloan Foundation.

[1]Y. Sato-Sorensen, J. Geophys. Res. **88**, 3543 (1983).
[2]F. Birch, J. Geophys. Res. **83**, 1257 (1978).
[3](a) S. Froyen and M. L. Cohen, Phys. Rev. B **29**, 3770 (1984); (b) M. Jackson, R. Hemley, and R. Gordon (unpublished).
[4]M. S. T. Bukowinski and J. Aidun (unpublished).
[5]H. K. Mao, P. M. Bell, K. J. Dunn, R. M. Chrenko, and R. C. Devries, Rev. Sci. Instrum. **50**, 1002 (1979).
[6]H. K. Mao, P. M. Bell, J. W. Shaner, and D. J. Steinberg, J. Appl. Phys. **49**, 3276 (1978); J. D. Barnett, S. Block, and G. J. Piermanini, Rev. Sci. Instrum. **44**, 1 (1973).
[7]R. Jeanloz, J. Geophys. Res. **86**, 6171 (1981).
[8]L. G. Liu and W. A. Bassett, J. Appl. Phys. **44**, 1475 (1973); W. A. Bassett and T. Takahashi, in *Advances in High Pressure Research,* edited by R. H. Wentdorf, Jr. (Academic, New York, 1974), p. 165.
[9]H. H. Demarest, Jr., C. R. Cassell, and J. C. Jamieson, J. Phys. Chem. Solids **39**, 1211 (1978).
[10]F. Birch, Phys. Rev. **71**, 809 (1947).
[11]R. Jeanloz, Geophys. Res. Lett. **8**, 1219 (1981).
[12]R. Jeanloz, in *High-Pressure Research in Geophysics,* edited by S. Akimoto and M. H. Manghanini (Center for Academic Publication, Tokyo, 1982), p. 479.
[13]Y. Sato and R. Jeanloz, J. Geophys. Res. **86**, 11, 773 (1981).
[14]R. Jeanloz and M. Roufosse, J. Geophys. Res. **87**, 10763 (1982).
[15]M. C. Roufosse and R. Jeanloz, J. Geophys. Res. **88**, 7399 (1983).
[16]Y. Sato-Sorenson (private communication).
[17]J. R. Hardy and A. M. Karo, *The Lattice Dynamics and Statics of Alkali Halide Crystals* (Plenum, New York, 1979).
[18]M. J. L. Sangster and M. Dixon, Adv. Phys. **25**, 247 (1976).
[19]Y. Ida, Phys. Earth Planet Int. **13**, 97 (1976).

[20]M. J. L. Sangster and R. M. Atwood, J. Phys. C **11**, 1541 (1978).
[21]J. Shanker and D. P. Agrawal, J. Phys. Chem. Solids **41**, 1001 (1980).
[22]D. W. Hafemeister and W. H. Flygare, J. Chem. Phys. **43**, 795 (1965).
[23]D. W. Hafemeister and J. D. Zahrt, J. Chem. Phys. **47**, 1428 (1967).
[24]E. H. Carlson, J. Chem. Phys. **58**, 1905 (1973).
[25]W. A. Harrison, *Electronic Structure* (Freeman, San Francisco, 1980).